



## OPEN ACCESS

EDITED BY  
Paula Schaiquevich,  
Garrahan Hospital, Argentina

REVIEWED BY  
Tyler Dunlap,  
University of North Carolina at Chapel  
Hill, United States  
Shawn D. Spencer,  
Philadelphia College of Osteopathic  
Medicine (PCOM), United States

\*CORRESPONDENCE  
Weize Huang,  
huang.weize@gene.com

†PRESENT ADDRESS  
Linzhong Li,  
Daiichi Sankyo, Inc., Basking Ridge, NJ,  
United States

SPECIALTY SECTION  
This article was submitted to Obstetric  
and Pediatric Pharmacology,  
a section of the journal  
Frontiers in Pharmacology

RECEIVED 21 June 2022  
ACCEPTED 29 August 2022  
PUBLISHED 26 September 2022

CITATION  
Huang W, Stader F, Chan P,  
Shemesh CS, Chen Y, Gill KL, Jones HM,  
Li L, Rossato G, Wu B, Jin JY and  
Chanu P (2022), Development of a  
pediatric physiologically-based  
pharmacokinetic model to support  
recommended dosing of atezolizumab  
in children with solid tumors.  
*Front. Pharmacol.* 13:974423.  
doi: 10.3389/fphar.2022.974423

COPYRIGHT  
© 2022 Huang, Stader, Chan, Shemesh,  
Chen, Gill, Jones, Li, Rossato, Wu, Jin  
and Chanu. This is an open-access  
article distributed under the terms of the  
[Creative Commons Attribution License  
\(CC BY\)](https://creativecommons.org/licenses/by/4.0/). The use, distribution or  
reproduction in other forums is  
permitted, provided the original  
author(s) and the copyright owner(s) are  
credited and that the original  
publication in this journal is cited, in  
accordance with accepted academic  
practice. No use, distribution or  
reproduction is permitted which does  
not comply with these terms.

# Development of a pediatric physiologically-based pharmacokinetic model to support recommended dosing of atezolizumab in children with solid tumors

Weize Huang<sup>1\*</sup>, Felix Stader<sup>2</sup>, Phyllis Chan<sup>1</sup>, Colby S. Shemesh<sup>1</sup>, Yuan Chen<sup>1</sup>, Katherine L. Gill<sup>2</sup>, Hannah M. Jones<sup>2</sup>, Linzhong Li<sup>2†</sup>, Gianluca Rossato<sup>3</sup>, Benjamin Wu<sup>1</sup>, Jin Y. Jin<sup>1</sup> and Pascal Chanu<sup>1</sup>

<sup>1</sup>Genentech Inc, South San Francisco, CA, United States, <sup>2</sup>Certara UK Limited, Sheffield, United Kingdom, <sup>3</sup>F. Hoffmann-La Roche Ltd, Basel, Switzerland

**Background:** Atezolizumab has been studied in multiple indications for both pediatric and adult patient populations. Generally, clinical studies enrolling pediatric patients may not collect sufficient pharmacokinetic data to characterize the drug exposure and disposition because of operational, ethical, and logistical challenges including burden to children and blood sample volume limitations. Therefore, mechanistic modeling and simulation may serve as a tool to predict and understand the drug exposure in pediatric patients.

**Objective:** To use mechanistic physiologically-based pharmacokinetic (PBPK) modeling to predict atezolizumab exposure at a dose of 15 mg/kg (max 1,200 mg) in pediatric patients to support dose rationalization and label recommendations.

**Methods:** A minimal mechanistic PBPK model was used which incorporated age-dependent changes in physiology and biochemistry that are related to atezolizumab disposition such as endogenous IgG concentration and lymph flow. The PBPK model was developed using both *in vitro* data and clinically observed data in adults and was verified across dose levels obtained from a phase I and multiple phase III studies in both pediatric patients and adults. The verified model was then used to generate PK predictions for pediatric and adult subjects ranging from 2- to 29-year-old.

**Results:** Individualized verification in children and in adults showed that the simulated concentrations of atezolizumab were comparable (76% within two-fold and 90% within three-fold, respectively) to the observed data with no bias for either over- or under-prediction. Applying the verified model, the predicted exposure metrics including  $C_{min}$ ,  $C_{max}$ , and  $AUC_{tau}$  were consistent between pediatric and adult patients with a geometric mean of pediatric exposure metrics between 0.8- to 1.25-fold of the values in adults.

**Conclusion:** The results show that a 15 mg/kg (max 1,200 mg) atezolizumab dose administered intravenously in pediatric patients provides comparable atezolizumab exposure to a dose of 1,200 mg in adults. This suggests that a dose of 15 mg/kg will provide adequate and effective atezolizumab exposure in pediatric patients from 2- to 18-year-old.

#### KEYWORDS

alveolar soft part sarcoma, atezolizumab, physiologically-based pharmacokinetic (PBPK) modeling, pediatric extrapolation, pediatric oncology, solid tumor, clinical pharmacology, quantitative pharmacology

## Introduction

Atezolizumab is a humanized immunoglobulin (IgG) 1 monoclonal antibody (mAb) that targets human programmed death–ligand 1 (PD-L1) expressed on immune cells and tumor cells, and blocks program death protein 1 (PD-1) mediated inhibitory signals (Akinleye and Rasool, 2019; FDA, 2021). Atezolizumab has been approved for use in multiple indications (e.g., small cell and non-small cell lung cancer, hepatocellular carcinoma, urothelial carcinoma, melanoma) across several countries due to its demonstrated anti-tumor activity and acceptable safety profile (EMA, 2021; FDA, 2021). In adults, the pharmacokinetic (PK) profile of atezolizumab exhibited linearity (for at least 21 days after a single IV dose) over a dose range of 1 mg/kg to 20 mg/kg, with a systemic clearance (CL) of 0.2 L/day, a volume of distribution at steady state ( $V_{SS}$ ) of 6.91 L, and a terminal half-life ( $t_{1/2}$ ) of 27 days (Herbst et al., 2014; Stroh et al., 2017; FDA, 2021). Demographics and baseline characteristics including body weight, sex, albumin levels, tumor burden, and treatment-emergent anti-drug antibody (ADA) status are statistically significant covariates for the PK parameters of atezolizumab. Nonetheless, these factors show no clinically significant effect on systemic exposure of atezolizumab and hence require no dose adjustment (FDA, 2021). In addition, multiple studies have shown that atezolizumab has flat exposure–efficacy and exposure–safety relationships across multiple indications and patient populations (Stroh et al., 2017; Morrissey et al., 2019; Liu et al., 2022). Atezolizumab has also been studied in pediatric patients (Shemesh et al., 2019; Georger et al., 2020). Following 15 mg/kg (maximum dose of 1,200 mg) once every 3 weeks (Q3W), atezolizumab steady-state exposure (AUC) in 12- to 18-year-old pediatric patients was comparable to that of adult patients who received 1,200 mg Q3W, while atezolizumab exposure trended lower in pediatric patients less than 12-year-old, although data are relatively limited (Shemesh et al., 2019; FDA, 2021).

Recently, atezolizumab was tested in patients with alveolar soft part sarcoma (ASPS). Preclinical models show that the PD-1/PD-L1 axis likely contributes to immunosuppression in ASPS, and isolated reports in ASPS patients treated with anti PD-1/PD-L1 agents showed complete responders with a subset of patients remaining disease-free for several years (Groisberg et al., 2017; Conley et al., 2018; Raj et al., 2018; Wilky et al., 2019). This study

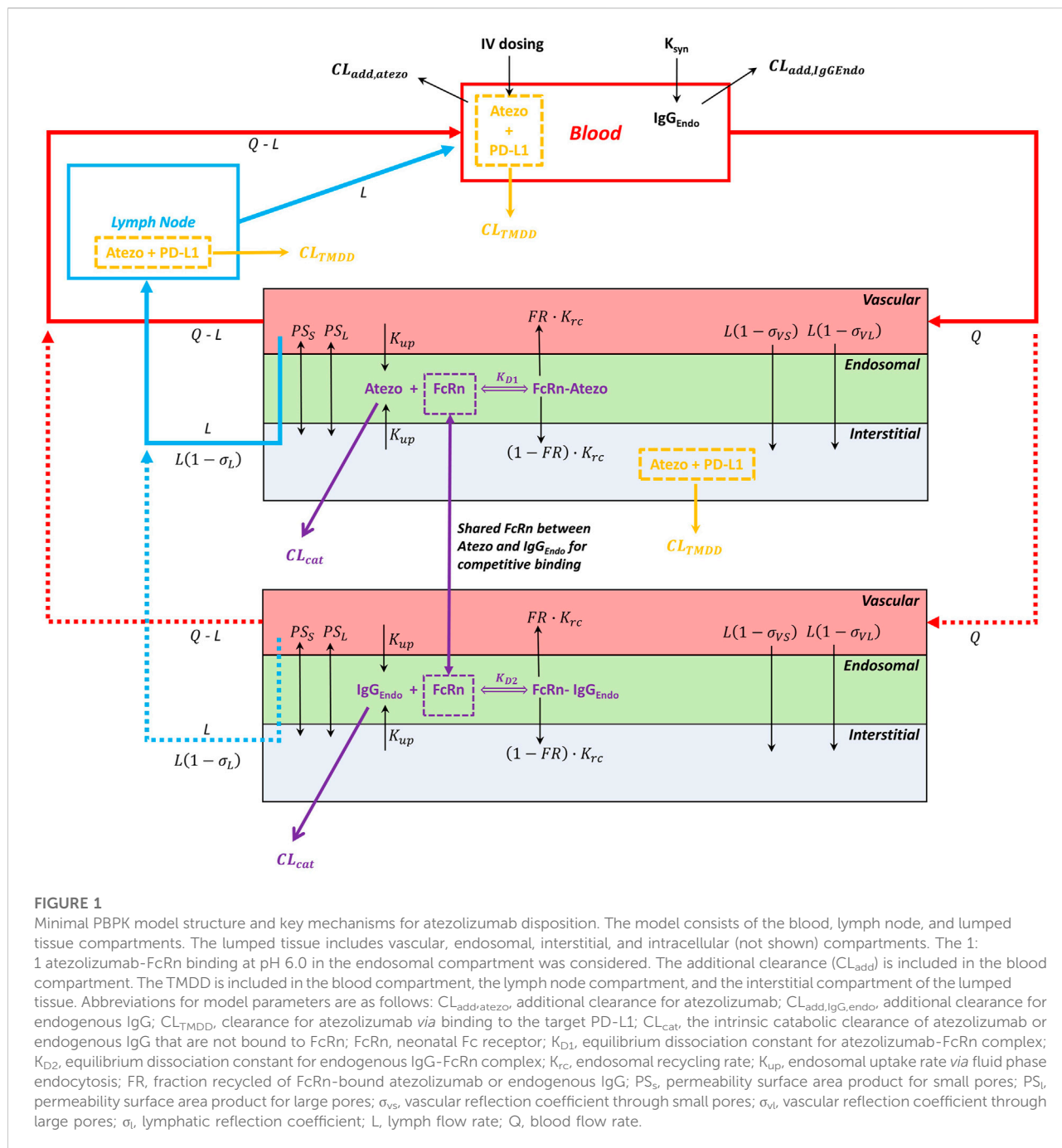
is a small multicenter open-label single-arm phase II trial for ASPS patients aged  $\geq 2$  years old. It includes patients with newly-diagnosed, unresectable, and metastatic disease (Naqash et al., 2021). In this study, atezolizumab was administered intravenously (IV) at a fixed dose of 1,200 mg in adults or at 15 mg/kg (1,200 mg maximum) Q3W in pediatric patients aged  $\geq 2$  years old. However, PK data were not obtained due to operational, ethical, and logistical challenges.

To better understand the PK of atezolizumab in pediatric patients, mechanistic PBPK modeling was used as it provides the advantage of incorporating age-dependent changes in physiology and biochemistry that are related to drug disposition (Edginton et al., 2006; Johnson et al., 2006). This approach has been verified with many small molecules (Huang et al., 2017; Lutz et al., 2021; Sinha et al., 2021; Zhu et al., 2021) and several therapeutic proteins (Li et al., 2014; Pan et al., 2020). In this study, we first developed an adult PBPK model using a combination of *in vitro* data and clinical human PK data after a single dose of 0.3 mg/kg and 20 mg/kg of atezolizumab (Herbst et al., 2014) and verified the model against other dose levels (Herbst et al., 2014) and data from additional studies (Stroh et al., 2017). Then, we implemented age-dependent maturation (Pan et al., 2020) and verified the pediatric model using individual PK data from 2- to 18-year-old patients (Shemesh et al., 2019; Georger et al., 2020). Finally, we used the verified model to generate simulations that enabled comparison of the atezolizumab PK across different age groups following 15 mg/kg atezolizumab to investigate exposure changes as pediatric subjects grow. The mechanistic PBPK model-based simulations allowed us to better understand atezolizumab exposure in children to support dose rationale and potentially label recommendations without sampling burden to pediatric patients for additional PK data.

## Material and methods

### Model structure and atezolizumab data sources

A minimal mechanistic PBPK model structure within the Simcyp Simulator version 20R1 (Simcyp Limited, Certara,



Sheffield, United Kingdom) was used for atezolizumab. This model structure has been verified previously to capture the systemic disposition of multiple antibody therapeutics (Li et al., 2014; Pan et al., 2020). It also allowed redefinition of the physiology of virtual subjects/population over the length of the simulation for pediatric populations. Briefly, the minimal PBPK model structure contains six compartments: 1) blood; 2) lymph node; and, a lumped tissue that is subdivided into 3) the vascular space, 4) the endosomal

space, 5) the interstitial space, and 6) the intracellular space. The model structure with mechanistic pathways is depicted in Figure 1 [adapted from (Li et al., 2014)] and related equations were previously described (Mager and Krzyzanski, 2005; Li et al., 2014; Gill et al., 2016; Pan et al., 2020). The clinical data of atezolizumab used in this model are mainly from three studies (Herbst et al., 2014; Stroh et al., 2017; Shemesh et al., 2019). The overall modeling strategy is illustrated in Figure 2 [adapted from (Huang et al., 2020)].

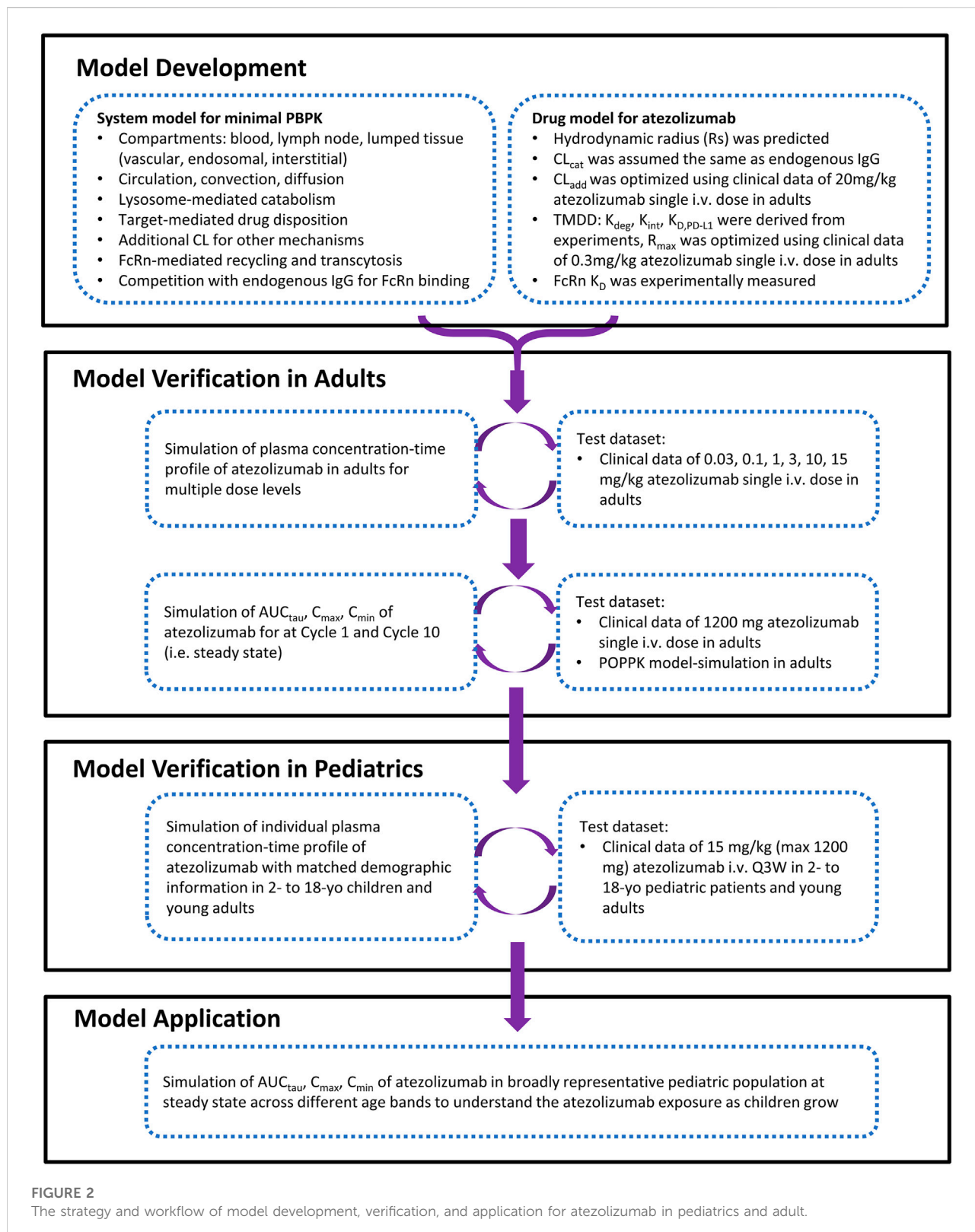


**FIGURE 2**  
The strategy and workflow of model development, verification, and application for atezolizumab in pediatrics and adult.

## Atezolizumab physiologically-based pharmacokinetic model development in adults

In this model, atezolizumab was administered intravenously. The distribution of atezolizumab was governed by circulation *via* blood and lymph flow, diffusion, and convection through pores in the endothelial wall, as well as transcytosis driven by endosomal uptake with subsequent binding to the neonatal Fc receptor (FcRn) and recycling to the vascular or interstitial compartments. The convection and diffusion of atezolizumab was predicted using the 2-pore hypothesis (Rippe and Haraldsson, 1987; Gill et al., 2016), which took into account the hydrodynamic radius ( $R_s$ ) of atezolizumab and size of the pores of the lumped tissue (i.e., the weighted average of pore sizes in all specific organs/tissues in the Simcyp full-body PBPK model). The parameter values of vascular reflection coefficient through small and large pores ( $\sigma_{vs}$  and  $\sigma_{vl}$ ) and permeability surface area product for small and large pores ( $PS_s$  and  $PS_l$ ) in the lumped tissue were calculated using a previously-described method (Rippe and Haraldsson, 1987; Aukland and Reed, 1993). Similar to many full-length IgG-like mAbs, atezolizumab also undergoes non-specific pinocytosis [i.e., endosomal uptake ( $K_{up}$ ), that eventually forms the acidified endosomal compartment (pH 6.0) where atezolizumab binds to FcRn [ $K_D$  value of 650 nM (Chung et al., 2019) with 1:1 binding stoichiometry] for protection from catabolic degradation ( $CL_{cat}$ ) and recycling ( $K_{rc}$ ). During this process, endogenous IgG and atezolizumab were modeled simultaneously to enable competition for FcRn binding in the endosomal space (Li et al., 2014). Endogenous IgG had a predicted  $R_s$  of 5.0 nm, a measured FcRn  $K_D$  value of 728 nM (Suzuki et al., 2010), a synthesis rate ( $K_{syn}$ ) of 0.64  $\mu\text{M}/\text{h}$ , an experimentally-based  $K_{up}$  of 0.0298 L/h (Haigler et al., 1979), an optimized  $K_{rc}$  value of 3.13 L/h, a lysosome-mediated  $CL_{cat}$  value of 0.0175 L/h (Li et al., 2014), and a  $CL_{add}$  value of 0.0017 L/h which encompassed elimination pathways such as Fc $\gamma$  receptor-mediated phagocytosis and degradation in non-FcRn-expressing cells. This model was calibrated to capture the known kinetics of endogenous IgG, the observed mean plasma endogenous IgG concentration around 80  $\mu\text{M}$  in adults, and the reduction of endogenous IgG level after IVIG administration and in FcRn deficient subjects. These FcRn-mediated mechanisms are particularly relevant to the pediatric population as endogenous IgG level is dependent on age (Allansmith et al., 1968; Aksu et al., 2006; Pan et al., 2020), in contrast to the relative constant level around 80  $\mu\text{M}$  in the adult population (Waldmann and Strober, 1969; Pan et al., 2020). For atezolizumab, the  $K_{up}$ ,  $K_{rc}$ , and fraction recycled (FR) values were assumed to be the same as for endogenous IgG, resulting in an estimated  $V_{SS}$  value of 0.066 L/kg.

Three atezolizumab clearance pathways were implemented: 1) target-mediated drug disposition (TMDD) through PD-L1 binding and subsequent elimination; 2) catabolism in the lysosome ( $CL_{cat}$ ); and 3) unspecified additional systemic clearance ( $CL_{add}$ ). The clearance pathways were optimized using a mixed bottom-up and top-down approach

(i.e., middle-out) leveraging both *in vitro* data and clinical data after high dose (minimal TMDD) and low dose (significant TMDD) treatment (Herbst et al., 2014). In this regard, the initial model used an *in vitro* FcRn  $K_D$  value for atezolizumab and default  $CL_{cat}$  (i.e., same as endogenous IgG) without  $CL_{add}$ , which resulted in overprediction of systemic exposure (Supplementary Figure S1). Thus, the model was calibrated by adjusting the  $CL_{add}$  value to ensure that the simulated plasma atezolizumab concentrations following a single dose of 20 mg/kg (the highest dose level was chosen to ensure the impact of TMDD on the overall clearance was minimal) could successfully recapitulate the observed data in adult patients with solid tumors and hematologic malignancies (Herbst et al., 2014).

As clinical data at dose level <1 mg/kg showed pronounced nonlinear PK (Herbst et al., 2014), the TMDD pathway was also incorporated into the adult atezolizumab PBPK model. Since PD-L1 exists as both a soluble and a membrane-bound receptor on immune cells located in blood, interstitial fluid, and lymph, the TMDD component was included into each of these compartments in the PBPK model. For the target, a median PD-L1 degradation rate constant ( $K_{deg}$ ) of 0.0426 L/h was calculated from values presented in multiple publications (Supplementary Table S1). A PD-L1 expression level ( $R_{max}$ ) value of 0.609 nM was fitted from clinical data in adult patients with solid tumor and hematological malignancy receiving 0.3 mg/kg atezolizumab (Herbst et al., 2014). A PD-L1  $K_{syn}$  value of  $2.59 \times 10^{-5} \mu\text{M}/\text{h}$  was then calculated from  $R_{max} \times K_{deg}$ . For the binding, a quasi-equilibrium model was used to describe the TMDD for atezolizumab, using a measured internalization rate constant ( $K_{int}$ ) value of 0.606 L/h determined from the percent of PD-L1 remaining at the cell surface as evaluated in the pancreatic cancer cell line BxPC-3 using flow cytometry analysis (Burr et al., 2017). Total PD-L1 was considered dynamic in the model due to its differing internalization and degradation rate constants. Equilibrium binding studies to determine atezolizumab  $K_D$  for PD-L1 were performed using three lots of atezolizumab and its chimeric derivative, PRO304397, with human PD-L1 expressed on 293 cells (EMA, 2021). Thus, a weighted mean  $K_D$  value of 0.299 nM was calculated from the reported *in vitro* values (Supplementary Table S2). Overall, four atezolizumab-specific parameters (FcRn  $K_D$ , PD-L1  $K_{deg}$ , PD-L1  $K_{int}$ , and PD-L1  $K_D$ ) were derived from experiments and two parameters were optimized ( $CL_{add}$  and  $R_{max}$ ) using human data. All final model parameters are shown in Table 1.

## Atezolizumab model verification in adults

To verify the model in adults, the simulated atezolizumab plasma concentration-time profiles following single dosing over a

TABLE 1 Parameter values for atezolizumab PBPK model.

Parameter	Value	References
Physicochemical parameters		
Molecular Weight (kDa)	145	FDA, (2021)
Hydrodynamic radius, $R_s$ (nm)	5.01	Predicted
B:P	0.55	Default
$f_{u,p}$	1	Default
Distribution parameters—minimal PBPK model—1:1 FcRn binding		
$K_{D1}$ ( $\mu$ M)	0.65	Chung et al. (2019)
$K_{up}$ (1/hr)	0.0298	Assumed to be the same as endogenous IgG
$K_{rc1}$ (1/hr)	3.13	Assumed to be the same as endogenous IgG
FR	0.5	Assumed to be the same as endogenous IgG
$\sigma_{v,s}$	0.9	Calculated
$\sigma_{v,l}$	0.16	Calculated
$PS_s$	0.0017	Calculated
$PS_l$	0.0029	Calculated
Elimination parameters		
$CL_{cat}$ (L/hr)	0.0175	Assumed to be the same as endogenous IgG
$CL_{add}$ (L/hr)	0.00693	Optimized
$CL_{lymph}$ (L/hr)	0	No binding to Fc $\gamma$ receptors and thus no macrophage clearance in the lymph is expected (Inman et al., 2017)
TMDD parameters—target		
PD-L1 $R_{max}$ ( $\mu$ M)	0.000609	Optimized
PD-L1 $K_{deg}$ (1/hr)	0.0426	Median value from meta-analysis (Supplementary Table S1)
PD-L1 $K_{syn}$ ( $\mu$ M/hr)	$2.59 \times 10^{-5}$	Calculated
PD-L1 molecular weight (Da)	33,275	<a href="https://www.phosphosite.org/proteinAction.action?id=19198&amp;showAllSites=true">https://www.phosphosite.org/proteinAction.action?id=19198&amp;showAllSites=true</a>
TMDD parameters—QE		
Target location	Plasma, lymph & interstitial	EMA Assessment Report (EMA, 2021)
$R_{max}$ option	Dynamic	Burr et al. (2017)
PD-L1 $K_D$ ( $\mu$ M)	0.000299	EMA Assessment Report (EMA, 2021)
PD-L1 $K_{int}$ (1/hr)	0.606	Burr et al. (2017)

667-fold dose range (0.03 mg/kg to 20 mg/kg) in adult patients with solid tumors and hematologic malignancies were compared to observed data (Herbst et al., 2014). The clinical data showed that atezolizumab exposure becomes dose proportional (i.e., linear PK) at dose levels >1 mg/kg (Herbst et al., 2014). Therefore, TMDD was expected to account for only a minor contribution to the overall clearance of atezolizumab at the relevant 15 mg/kg dose in pediatric patients. To confirm this, simulations were performed in adults and pediatrics receiving 15 mg/kg atezolizumab, including and excluding the TMDD component. Comparable PK was observed (Supplementary Figure S2), therefore TMDD was not included in the subsequent modeling and simulations. The PBPK model without the TMDD component was further verified by

comparing the simulated atezolizumab exposure metrics in adult patients with observed data following a single dose of 1,200 mg and simulated data at steady state from the published population pharmacokinetic (PopPK) model following multiple dosing of 1,200 mg Q3W (Stroh et al., 2017) (Supplementary Table S3).

## Atezolizumab physiologically-based pharmacokinetic model development in pediatric patients

After the atezolizumab PBPK model for adults was developed and verified, age-dependent physiological and

biochemical changes in tissue volumes (vascular, endosomal, interstitial, and intracellular), blood and lymph flows, hematocrit, and endogenous IgG concentration were incorporated as described previously (Johnson et al., 2006; Johnson and Rostami-Hodjegan, 2011; Pan et al., 2020) to establish the pediatric atezolizumab PBPK model. Notably, the ontogeny of endogenous IgG concentration was described by combining maternal and pediatric contributions using an exponential decline for maternal IgG and a saturable function for the increasing pediatric contribution (Pan et al., 2020). A quantitative measure of FcRn ontogeny is currently lacking in the literature, therefore the mean FcRn concentration in pediatric subjects was assumed the same as in adults. To capture interindividual variability, the FcRn concentration in each pediatric subject was calculated based upon the correlation with endogenous IgG (Li et al., 2014; Pan et al., 2020). When this correlation was enabled, the model predicted a reasonable variability in exogenous IgG  $t_{1/2}$  and captured the trajectory of exogenous IgG  $t_{1/2}$  in pediatric subjects in relation to endogenous IgG level (Pan et al., 2020). The ontogeny data of lymph flow were not available. Therefore, adult lymph flow was scaled allometrically with an exponent of 0.75 for pediatric subjects, resulting in a total lymph flow that was 2.6-fold higher in neonates than in adults (Pan et al., 2020). The percentage of total lymph flow coming from each specific organ/tissue was assumed the same in children as in adults (Gill et al., 2016). The potential changes of  $CL_{cat}$  and  $CL_{add}$  during pediatric growth was assumed to follow body weight-based allometric scaling with an exponent of 0.808, which was determined from a PopPK model (Stroh et al., 2017). This value was similar to the allometric exponent (0.81) published from an analysis of data for 23 mAbs in humans and cynomolgus monkeys (Betts et al., 2018). Since the ontogeny of PD-L1 in children was unknown and the high atezolizumab concentration after a dose of 15 mg/kg likely fully saturates the target, the model without TMDD was used for pediatric simulation and extrapolation. To test the validity of the exclusion of TMDD, simulations were performed in both adult and pediatric populations receiving 15 mg/kg atezolizumab, both including and excluding the TMDD model, and the predicted atezolizumab exposure was not significantly affected (Supplementary Figure S2).

## Individualized model verification in pediatric patients

To verify the model in pediatrics, the physiology of the simulated virtual pediatric subjects was redefined at regular intervals over the length of simulation based on the age, as the physiology of virtual pediatric subjects developed significantly during the simulation time. The redefining schedule was every

2 weeks for 2- to 6-year-old subjects and every month for >6-year-old subjects. These schedules were selected in order to seamlessly predict PK concurrent with subject maturation and resulted in a discrepancy <2% in all relevant physiological parameters (Abduljalil et al., 2014). An individualized model verification approach was used to evaluate the atezolizumab model in both pediatric patients and in adult patients. The simulated plasma atezolizumab concentrations for each virtual subject matching the enrolled patient's unique age, sex, and dose regimen were compared with observed sparse sampling data obtained following multiple dosing (Q3W) of atezolizumab 15 mg/kg in 2- to 18-year-old pediatric patients and 1,200 mg in 18- to 29-year-old adult patients for up to 672 days (Shemesh et al., 2019). The simulated body weight distribution from virtual subjects was also compared to the actual body weight of enrolled patients because of the 15 mg/kg body weight-based dosing (Supplementary Figure S3).

## Physiologically-based pharmacokinetic model applications

Simulations until steady state were produced using the verified PBPK model for broadly representative virtual subjects from 2 to 18 years old after 15 mg/kg (not exceeding 1,200 mg) and subjects  $\geq 18$  years old after 1,200 mg IV atezolizumab. The age range of interest (2 to <18 yo) was stratified into 3 age bands: 2 to <6 yo, 6 to <12 yo, and 12 to <18 yo. Ten virtual trials of 20 pediatric subjects (50% female) for each age band was used as the simulation set-up. The values, statistics, and distributions of  $C_{min}$ ,  $C_{max}$ , and  $AUC_{tau}$  after the first (cycle 1) and steady state (cycle 10) dose were derived.

## Sensitivity analysis

A sensitivity analysis was performed to evaluate the sensitivity of the simulated atezolizumab exposure to the individual clearance pathways implemented in the PBPK model. Atezolizumab exposure was simulated ( $C_{min}$ ,  $C_{max}$ , and  $AUC_{tau}$ ) following a single dose and at steady state (15 mg/kg Q3W in children and 1,200 mg Q3W in adults) in 2- to 4-, 4- to 8-, 8- to 12-, and 12- to 18-year-old pediatric patients and in adult patients where only  $CL_{cat}$  or  $CL_{add}$  was included in the PBPK model.

Additionally, the impact of key parameters ( $K_{up}$ ,  $K_{rc}$ , and FcRn abundance) on plasma atezolizumab concentration profile and systemic AUC was tested individually with other model parameters kept constant. The tested parameter range of  $K_{up}$ ,  $K_{rc}$ , and FcRn abundance was 0.000298–2.98  $h^{-1}$ , 0.0313–313  $h^{-1}$ , and 0.1–1,000  $\mu M$ , respectively.

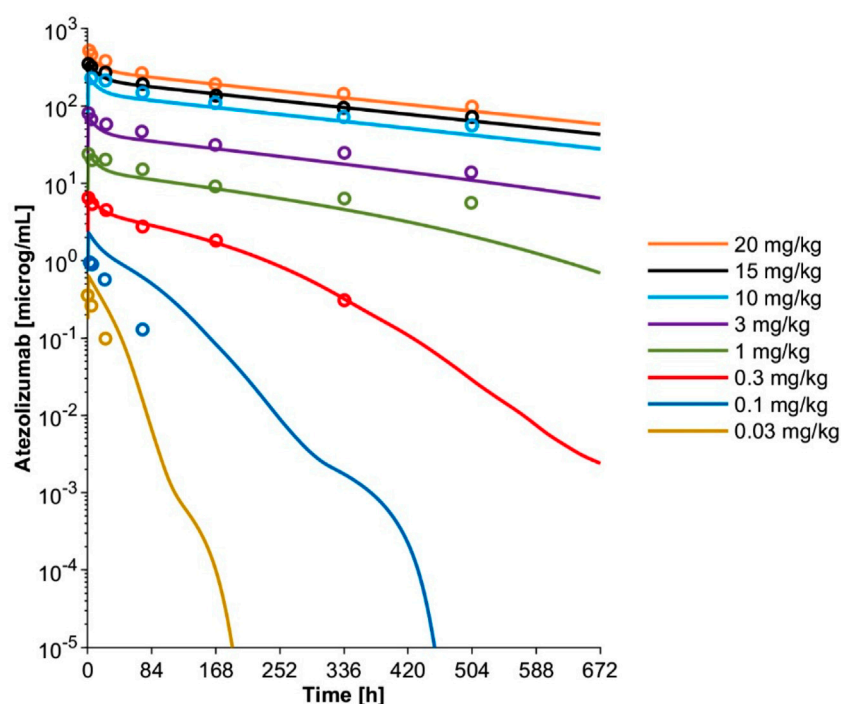


**FIGURE 3**

Simulated mean plasma concentration-time profiles and observed mean concentration data for adult patients with solid tumors and hematologic malignancies after a single IV dose at varying dose levels using the optimized final PBPK model including TMDD. Observed mean data are shown as open circles (Herbst et al., 2014). Simulated mean data are shown as solid lines.

## Results

### Physiologically-based pharmacokinetic model development and verification in adults

The initial model with only lysosome based  $CL_{cat}$  overpredicted atezolizumab exposure compared to the clinical data after treatment with 20 mg/kg (Supplementary Figure S1A) (Herbst et al., 2014). Thus,  $CL_{add}$  was included and optimized as 0.00693 L/h to improve model performance and recapitulate the clinically observed data (Supplementary Figure S1B). The model with both  $CL_{cat}$  and  $CL_{add}$  overpredicted drug exposure at lower dose levels (Supplementary Figure S1C), necessitating the inclusion of a TMDD component, where PD-L1 target expression ( $R_{max}$ ) was optimized as 0.609 nM to recover the clinically observed data after receiving 0.3 mg/kg (Supplementary Figure S1D). The final TMDD model was then verified over a dose range of 0.03 to 20 mg/kg, where the atezolizumab concentration-time profiles at all dose levels were adequately captured (Figure 3). This confirmed that the minimal PBPK model with TMDD was able to successfully describe atezolizumab disposition in adults.

The TMDD pathway was excluded for pediatric patient modeling due to the minimal contribution of TMDD to atezolizumab disposition at the 15 mg/kg dose level and the

lack of ontogeny data on the PD-L1 target. Simulations including and excluding the TMDD component were performed in adult and pediatric patients receiving a 15 mg/kg dose of atezolizumab to confirm that the exclusion of TMDD had minimal impact. These results showed that the predicted plasma atezolizumab concentration-time profile was not significantly different when TMDD was included or excluded (Supplementary Figure S2). The PBPK model without the TMDD component was further verified by comparing the simulated atezolizumab exposure metrics for adult patients with observed data following a single dose of 1,200 mg from a separate dataset (Stroh et al., 2017) as well as simulated data at steady state from a published PopPK model following multiple dosing of 1,200 mg Q3W (Stroh et al., 2017) (Supplementary Table S3). This comparison revealed that the simulated atezolizumab exposure metrics including  $C_{min}$ ,  $C_{max}$ , and  $AUC_{tau}$  from the PBPK model without TMDD all agreed with both observed data and the PopPK model-simulated data after both single dosing and multiple dosing at cycle 1 and after cycle 10. Taken together, we showed that the TMDD pathway did not play a significant role in atezolizumab disposition at therapeutic dose levels; the minimal PBPK model without TMDD was successfully verified to capture atezolizumab PK after IV administration of 15 mg/kg in adults, which was considered for the subsequent modeling in pediatrics.

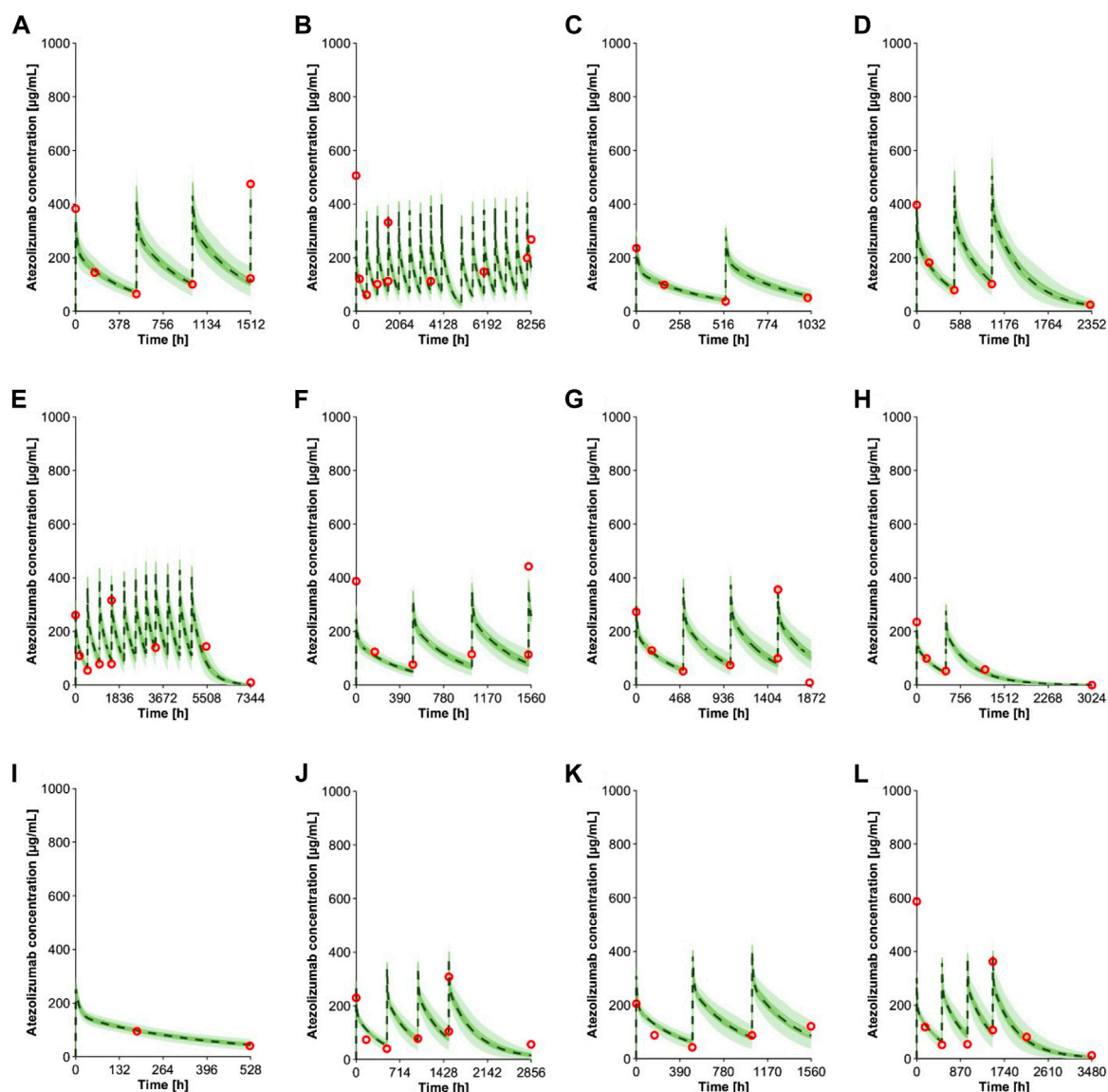


**FIGURE 4**

Individual observed plasma concentrations (Shemesh et al., 2019) and simulations of multiple IV doses of 15 mg/kg (<18 yo) or 1,200 mg ( $\geq 18$  yo) atezolizumab Q3W in pediatrics. The panels show data from subjects with different age (A) 16 yo, (B) 15 yo, (C) 13 yo, (D) 12 yo, (E) 11 yo, (F) 10 yo, (G) 8 yo, (H) 7 yo, (I) 5 yo, (J) 4 yo, (K) 3 yo, and (L) 2 yo. Observed data (Shemesh et al., 2019) are shown in red open circles. The green lines represent simulated trials, and the dashed black lines represent the mean data for the entire simulated population ( $n = 100$ ). The green shaded area represents the 5th to 95th percentiles of the simulations.

## Physiologically-based pharmacokinetic model development and individualized verification in pediatrics

The virtual pediatric population in the Simcyp V20 was selected for pediatric modeling after the atezolizumab PBPK model was developed and verified for adults. An individualized model verification approach was used to evaluate the atezolizumab model for both pediatric subjects and young adults using individual observed data from every

single enrolled subject (Shemesh et al., 2019). The virtual subjects in the model were matched to have the same age and gender as enrolled patients with comparable body weight (Supplementary Figure S3). The simulated concentration-time profiles adequately recovered the observed longitudinal data following multiple IV doses of atezolizumab (15 mg/kg in <18-year-olds and 1,200 mg  $\geq 18$ -year-olds Q3W; representative data shown in Figure 4). A comparison of all simulated and observed plasma atezolizumab concentrations ( $N = 431$ ) from 87 subjects is shown in Figure 5, stratified by age group (0–6 years, 6–12 years,

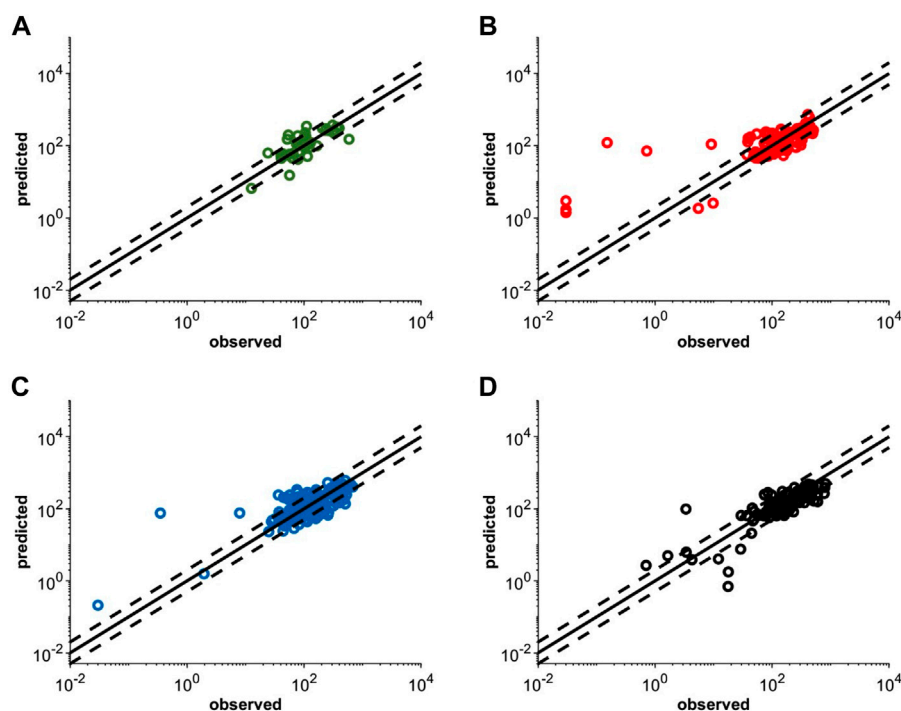


**FIGURE 5**

Individualized simulated mean and observed (Shemesh et al., 2019) plasma concentrations following multiple IV doses of 15 mg/kg (<18 yo) or 1,200 mg ( $\geq$ 18 yo) atezolizumab Q3W in pediatric patients (A) 0–6 yo, (B) 6–12 yo, and (C) 12–18 yo or (D) young adult patients with solid tumors and hematologic malignancies. The solid black lines represent the line of unity and the dashed black lines represent the 2-fold error margin. Each simulation matched the dosing information and demographics with each enrolled subject.

12–18 years, and 18–29 years). Overall, the simulated concentrations of atezolizumab were comparable (76% within two-fold and 90% within three-fold) to the observed data (Supplementary Table S4). There was no bias for either over- or underprediction, and prediction accuracy was similar across the age range (Supplementary Table S4; Figure 5). Notably, the accuracy was relatively reduced at the lower concentrations, which represented samples taken a long time after the final dose (Figure 5). Overall, the model performance indicates successful verification of the pediatric atezolizumab PBPK model.

## Physiologically-based pharmacokinetic model applications

After individualized verification for pediatric patients, the model was applied to produce simulations until steady state in a representative virtual population. The distribution of exposure metrics including  $C_{min}$ ,  $C_{max}$ , and  $AUC_{tau}$  were not significantly different between children and adults (Figure 6), with a geometric mean of pediatric exposure metrics between 0.8- to 1.25-fold of adult value (Table 2), although slightly lower  $C_{min}$ ,  $C_{max}$ , and  $AUC_{tau}$  were observed in pediatric subjects. At both Cycle 1 and at steady state (Cycle 10), no pediatric subjects were predicted to

have a  $C_{max}$  outside of the acceptable adult criteria (50%–200% of the adult median value) (Figure 6; Supplementary Table S5). For Cycle 1,  $C_{min}$  values were predicted to be <50% of the adult median value in 11.5%, 11.0%, and 11.5% of subjects aged 2- to 6-year-old, 6- to 12-years old, and 12- to 18-year-old, respectively; no subjects were predicted to be >200% adult median value in any age group. At steady state (Cycle 10),  $C_{min}$  values were predicted to be <50% of the adult median value in 10.5%, 10.0%, and 10.5% of subjects and >200% adult median value in 4.0%, 1.0%, and 0.5% of subjects aged 2- to 6-year-old, 6- to 12-years old, and 12- to 18-year-old, respectively (Supplementary Table S6). No pediatric subjects were predicted to have a Cycle 1  $C_{min}$  <6  $\mu$ g/ml, which was the minimal effective concentration (Deng et al., 2016). For Cycle 1,  $AUC_{tau}$  values were predicted to be <50% of the adult median value in 0.5% of subjects aged 2- to 6-year-old and 6- to 12-year-old, and no subjects aged 12- to 18-year-old. At steady state,  $AUC_{tau}$  values were predicted to be <50% of the adult median value in 1.5%, 1.5%, and 2.5% of subjects aged 2- to 6-year-old, 6- to 12-year-old, and 12- to 18-year-old, respectively (Supplementary Table S7). No pediatric subjects were predicted to have an  $AUC_{tau}$  greater than the adult acceptable criteria (200% of the adult median value) following a single dose or at steady state. Overall, similar atezolizumab exposure was observed in pediatric patients

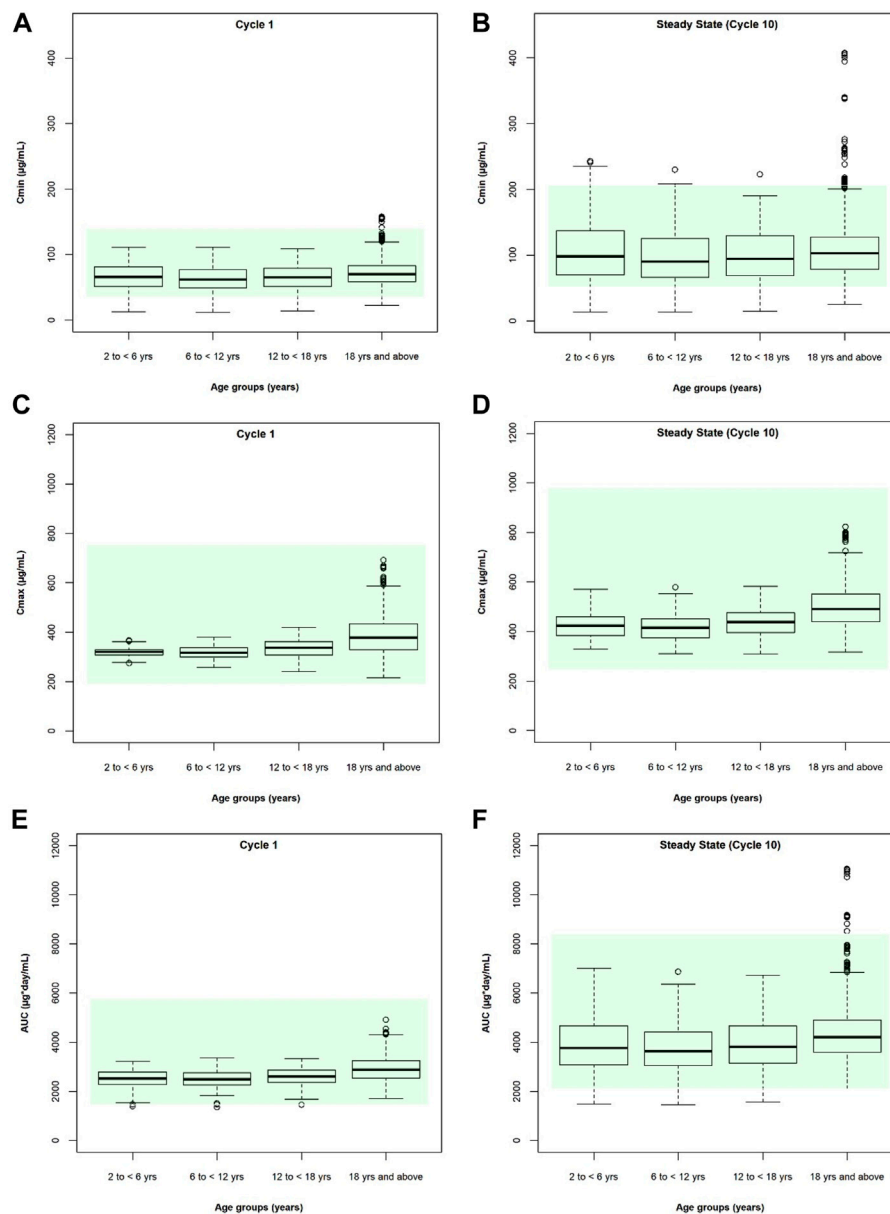


**FIGURE 6**

Cycle 1 and steady state (cycle 10) simulated atezolizumab (A,B)  $C_{min}$ , (C,D)  $C_{max}$ , and (E,F)  $AUC_{tau}$  for pediatric (2–6 yo, 6–12 yo, and 12–18 yo) and adult ( $\geq 18$  yo) patients following multiple IV doses of 15 mg/kg (<18 yo) or 1,200 mg ( $\geq 18$  yo) atezolizumab Q3W. The box represents the median value and interquartile range; error bars represent the 5th and 95th percentiles. Circles represent individual subjects outside of the 5th to 95th percentiles. Shaded area represents the simulated adult acceptable criteria (50%–200% of the adult median value).

regardless of age when compared with adults at both Cycle 1 and at steady state.

## Sensitivity analysis

As the simulated atezolizumab exposure was relatively flat over the 2–18 year age range, a sensitivity analysis was performed

to investigate the impact of each clearance pathway. When the PBPK model included only clearance *via* catabolism within the lysosomes ( $CL_{cat}$ ), exposure at steady state increased as age decreased; particularly, the impact is most pronounced for 2- to 12-yo children (Supplementary Figure S4). This reflects the impact of lower IgG levels in children, which results in reduced competition for binding to FcRn, more efficient recycling, less catabolism, and hence higher drug exposure. In contrast, when

TABLE 2 Predicted geometric mean plasma  $C_{min}$ ,  $C_{max}$ , and  $AUC_{tau}$  values for atezolizumab following multiple IV doses of 15 mg/kg atezolizumab Q3W in pediatric subjects and 1,200 mg in adults for Cycle 1 and Cycle 10 (steady state). Relative values of pediatric exposure metrics compared to adults are also shown.

Cycle		$C_{min}$ ( $\mu\text{g/ml}$ )	$C_{max}$ ( $\mu\text{g/ml}$ )	$AUC_{tau}$ ( $\mu\text{g} \times \text{day/ml}$ )	$C_{min}$	$C_{max}$	$AUC_{tau}$
					Relative to adult		
1	$\geq 18$ yo (adult)	68.2	380	2,894	1.00	1.00	1.00
	2 to 6 yo	62.2	319	2,483	0.91	0.84	0.86
	6 to 12 yo	59.3	316	2,464	0.87	0.83	0.85
	12 to 18 yo	60.8	333	2,557	0.89	0.88	0.88
10	$\geq 18$ yo (adult)	100	492	4,187	1.00	1.00	1.00
	2 to 6 yo	93.4	423	3,737	0.94	0.86	0.89
	6 to 12 yo	87.7	414	3,612	0.88	0.84	0.86
	12 to 18 yo	89.3	434	3,730	0.90	0.88	0.89

the PBPK model included only clearance *via* unspecified additional clearance ( $CL_{add}$ ), exposure decreased as age decreased (Supplementary Figure S5), due to the allometric exponent of 0.808 (Stroh et al., 2017) being applied to  $CL_{add}$  within the model, leading to higher clearance per kg in younger children that typically have lower body weight. When considering  $CL_{cat}$  and  $CL_{add}$  together in the final PBPK model, the total clearance resulted in a flat exposure predicted over the 2–18 year age range.

In addition, the effect of each of the key optimized parameters ( $K_{up}$ ,  $K_{rc}$ , and FcRn abundance) on plasma atezolizumab concentration profile and systemic AUC was tested. The current values of these parameters are within the sensitive ranges where simulation results may fluctuate significantly as the parameter value changes (Supplementary Figure S6). As  $K_{up}$  increases, systemic AUC decreases due to more endocytosis and subsequent catabolism. In contrast, as  $K_{rc}$  increases, systemic AUC increases due to more drug recycling and rescue from catabolism. Finally, as FcRn increases, the systemic AUC also increases due to increased binding to FcRn and protection from catabolism.

## Discussion

In this study, we developed a mechanistic PBPK model for atezolizumab (Figures 1, 2) using both *in vitro* and *in vivo* data and verified our model for adults (Figure 3; Table 1). We then incorporated maturation and verified the model for pediatric patients using individual clinically observed data from 87 children and young adults aged from 0 to 29 years old (Figures 4, 5). The verification showed unequivocally that our model was able to recapitulate atezolizumab disposition in both adult and pediatric populations. The verified model was then

applied to generate simulations in the broadly representative virtual populations across all age groups. The results indicated that atezolizumab exposure was comparable between children from 2- to 18-year-old following IV administration of 15 mg/kg (max 1,200 mg) atezolizumab Q3W and adults after 1,200 mg IV Q3W (Figure 6; Table 2), supporting our 15 mg/kg dose recommendation for atezolizumab in pediatric patients.

To date, pediatric studies are required when new molecular entities are being developed unless waived or deferred (Johnson and Ke, 2021). It is critical to understand the efficacy, safety, tolerability, and PK of drugs in children for appropriate and optimal drug utilization. However, blood samples may only be sporadically collected from pediatric patients to study the PK in this population because of the burden to children, blood sample volume limitation, and other logistical challenges (Abdel-Rahman et al., 2007; Joseph et al., 2015). Thus, there exists a need for the use of PK modeling and simulation techniques to understand and predict PK in children. This can facilitate safe and effective first-in-child dose design, supplement limited exposure data in children and support pediatric dosing recommendations.

Generally, dose recommendations in pediatric patients leverage empirical allometric scaling or mechanistic PBPK modeling (Germovsek et al., 2021; Johnson and Ke, 2021). The former approach uses power functions to calculate the drug clearance or volume of distribution based on the normalized body weight or body surface area of a pediatric subject with respect to an adult. In contrast, mechanistic PBPK models represent the biological system and consider age-dependent changes of physiology, anatomy, and biochemistry that together govern the drug disposition in the human body (Edginton et al., 2006; Johnson et al., 2006). The PBPK model provides a unique advantage over allometric scaling because all physiologically important components and

pathways are integrated within one framework in an inter-dependent and non-linear fashion. Furthermore, the maturation effect on drug disposition is derived as an aggregate of changes in each individual mechanism, which better represents the reality and complexity of the human system and system-drug interactions.

Over the past decade, the application of PBPK modeling in pediatric extrapolation has gained critical mass, particularly in small molecules (Huang et al., 2017; Lutz et al., 2021; Sinha et al., 2021; Zhu et al., 2021; Johnson et al., 2022), and regulatory agencies have shown general endorsement of such application (Luzon et al., 2017; Grimstein et al., 2019; Yellepeddi et al., 2019; Johnson and Ke, 2021). The rise of model-informed drug development initiatives provides a regulatory pathway for engaging pharmaceutical companies with the FDA, which allows for the incorporation of scientific findings and discussions into pediatric drug development with better transparency, alignment, and efficiency (Madabushi et al., 2019; Wang et al., 2019; Zhu et al., 2019).

However, the use of PBPK modeling in pediatrics is reported much less for mAbs when compared with small molecules. Thus, the applicability of the PBPK model for mAbs has not been extensively evaluated. One reason for this could be that mAbs represent a relatively newer modality and the number of marketed mAbs is considerably less than the number of small molecule drugs. Moreover, the mechanism of distribution and clearance differ dramatically between mAbs and small molecules, so previous knowledge of small molecules (e.g., the ontogeny profile of drug metabolizing enzymes) may not be relevant or applicable to mAbs. A significant knowledge gap of ontogeny exists in mechanisms specifically influencing the PK of mAbs such as transcytosis, FcRn expression, and lysosome-mediated degradation (Malik and Edginton, 2018; Malik and Edginton, 2020; Temrikar et al., 2020), where assumptions on the maturation and calibration using clinical data are needed to perform PBPK modeling and simulation. In spite of these challenges, six pediatric PBPK studies were recently conducted for more than ten biologics using either full-body or minimal structure using Simcyp or PK-Sim platforms (Hardiansyah and Ng, 2018; Hanke et al., 2019; Malik and Edginton, 2019; Basu et al., 2020; Malik and Edginton, 2020; Pan et al., 2020). Although these studies showed acceptable model performance, inconsistent approaches were utilized in order to capture PK of different drugs. To date, no consensus has been reached regarding the best methodology for PBPK modeling in pediatric patients for biologics.

In this study, our results indicated that atezolizumab exposure was comparable in subjects from 2 to 18 years old following IV administration of 15 mg/kg (max 1,200 mg) atezolizumab (Figure 6; Table 2). The reason for the flat exposure independent of age was mainly due to the cancellation of maturation effects on two separate clearance pathways: catabolism and unspecified additional clearance. The atezolizumab PBPK model considered changes in IgG

concentrations and competitive binding to FcRn. Following birth, the IgG levels in children first drop as maternal IgG is eliminated and reach a nadir concentration around month three to four, after which IgG concentrations start to increase due to *de novo* synthesis of their own IgG, gradually reaching a plateau at the age of 8–10 years (Allansmith et al., 1968; Aksu et al., 2006; Pan et al., 2020). This results in less competition for FcRn binding and more efficient recycling of mAbs, which leads to diminished drug catabolism in younger children when IgG levels are low. On the other hand, the unspecified additional clearance ( $CL_{add}$ ) was scaled with a PopPK model-estimated exponent of 0.808 on body weight (Stroh et al., 2017) causing a higher  $CL_{add}$  per kg in younger children. Our sensitivity analyses show that the atezolizumab exposure in children would have been higher or lower if only  $CL_{cat}$  or  $CL_{add}$  was included in the model, respectively (Supplementary Figures S4, S5).

This study has several limitations. Quantitative measure of the ontogeny profile for lymph flow and FcRn are lacking in humans. To account for the real-time growth, the changes in lymph flow in the pediatric PBPK model were based on an allometric approach to be consistent with data reported in pre-clinical species (Pan et al., 2020). For FcRn, the concentration was assumed to be the same between children and adults. However, a correlation method was used between individual FcRn and endogenous IgG concentration as described before (Pan et al., 2020), which successfully captured the changes in exogenous IgG terminal half-life when administered to children of different ages. The model does not account for target binding in pediatric patients and the ontogeny of PD-L1 in children is unknown. For this reason, the model is only suitable for prediction of therapeutic dose levels in pediatric patients, where TMDD is saturated and only has minimal impact on PK. In addition, development of anti-drug antibody (ADA) was not considered in the current model. Based on findings from iMATRIX study (Geoerger et al., 2020), the observed ADA incidence rate in pediatrics was 15% (9/60) which was less than or similar to that of the typical ADA incidence in adults in various indications (Shemesh et al., 2019). Lastly, we implemented an additional clearance ( $CL_{add}$ ) as an unspecified pathway for unknown mechanisms, which did not incorporate any ontogeny and might not be accurately captured in children. Because the  $CL_{add}$  was optimized empirically and minimal PBPK model was used, there is a potential risk that this parameter was overleveraged, which may be mitigated upon obtaining more mechanistic understanding of atezolizumab or applying a full body PBPK model. So far, the applicability of the Simcyp platform to biologics prediction in pediatrics has only been verified for six drugs and the confidence in 0- to 2-year-old population remains low (Pan et al., 2020). For atezolizumab, PK data from 0- to 2-year-old population

were only available in two subjects (Shemesh et al., 2019). More modeling and simulation studies along with more pediatric PK data are necessary to obtain higher confidence in the model applicability. As we acquire more knowledge, the PBPK model framework will be updated as an iterative process together with more pediatric data and simulation case studies.

In conclusion, the application of mAb PBPK model offers much promise, and this work allowed us to understand the atezolizumab exposure at the dose level of 15 mg/kg in pediatric patients from 2- to 18-year-old with solid tumors in relation to adults. These findings support the optimal and safe use of atezolizumab at this dose level for label recommendation.

## Data availability statement

The original contributions presented in the study are included in the article/Supplementary Material, further inquiries can be directed to the corresponding author.

## Author contributions

WH, PChan, CS, YC, JJ, and PChanu: study conception and design. WH, FS, PChan, CS, KG, LL, and PChanu: performing analysis and results interpretation. WH, FS, PChan, CS, YC, KG, HJ, LL, GR, BW, JJ, and PChanu: manuscript writing.

## Funding

This work was funded by Genentech Inc./Roche. The funder was involved in the study design and publication.

## References

- Abdel-Rahman, S. M., Reed, M. D., Wells, T. G., and Kearns, G. L. (2007). Considerations in the rational design and conduct of phase I/II pediatric clinical trials: Avoiding the problems and pitfalls. *Clin. Pharmacol. Ther.* 81, 483–494. doi:10.1038/sj.clpt.6100134
- Abduljalil, K., Jamei, M., Rostami-Hodjegan, A., and Johnson, T. N. (2014). Changes in individual drug-independent system parameters during virtual paediatric pharmacokinetic trials: Introducing time-varying physiology into a paediatric PBPK model. *AAPS J.* 16, 568–576. doi:10.1208/s12248-014-9592-9
- Akinleye, A., and Rasool, Z. (2019). Immune checkpoint inhibitors of PD-L1 as cancer therapeutics. *J. Hematol. Oncol.* 12, 92. doi:10.1186/s13045-019-0779-5
- Aksu, G., Genel, F., Koturoglu, G., Kurugol, Z., and Kutukculer, N. (2006). Serum immunoglobulin (IgG, IgM, IgA) and IgG subclass concentrations in healthy children: A study using nephelometric technique. *Turk. J. Pediatr.* 48, 19–24.
- Allansmith, M., McClellan, B. H., Butterworth, M., and Maloney, J. R. (1968). The development of immunoglobulin levels in man. *J. Pediatr.* 72, 276–290. doi:10.1016/s0022-3476(68)80324-5
- Aukland, K., and Reed, R. K. (1993). Interstitial-lymphatic mechanisms in the control of extracellular fluid volume. *Physiol. Rev.* 73, 1–78. doi:10.1152/physrev.1993.73.1.1
- Basu, S., Lien, Y. T. K., Vozmediano, V., Schlender, J. F., Eissing, T., Schmidt, S., et al. (2020). Physiologically based pharmacokinetic modeling of monoclonal antibodies in pediatric populations using PK-sim. *Front. Pharmacol.* 11, 868. doi:10.3389/fphar.2020.00868
- Betts, A., Keuncke, A., Van Steeg, T. J., Van Der Graaf, P. H., Avery, L. B., Jones, H., et al. (2018). Linear pharmacokinetic parameters for monoclonal antibodies are similar within a species and across different pharmacological targets: A comparison between human, cynomolgus monkey and hFcRn Tg32 transgenic mouse using a population-modeling approach. *MAbs* 10, 751–764. doi:10.1080/19420862.2018.1462429
- Burr, M. L., Sparbier, C. E., Chan, Y. C., Williamson, J. C., Woods, K., Beavis, P. A., et al. (2017). CMTM6 maintains the expression of PD-L1 and regulates anti-tumour immunity. *Nature* 549, 101–105. doi:10.1038/nature23643
- Chung, S., Nguyen, V., Lin, Y. L., Lafrance-Vanasse, J., Scales, S. J., Lin, K., et al. (2019). An *in vitro* FcRn-dependent transcytosis assay as a screening tool for predictive assessment of nonspecific clearance of antibody therapeutics in humans. *MAbs* 11, 942–955. doi:10.1080/19420862.2019.1605270
- Conley, A. P., Trinh, V. A., Zobniw, C. M., Posey, K., Martinez, J. D., Arrieta, O. G., et al. (2018). Positive tumor response to combined checkpoint inhibitors in a patient with refractory alveolar soft Part Sarcoma: A case report. *J. Glob. Oncol.* 4, 1–6. doi:10.1200/JGO.2017.009993

## Acknowledgments

The authors would like to thank Kit Wun Kathy Cheung and Kenta Yoshida for reviewing the manuscript, and Anshin BioSolutions, Inc. for editorial support.

## Conflict of interest

Authors WH, PChan, CS, YC, BW, JJ, Pchanu are salaried employees and stockholders of Genentech, Inc. FS, KG, HJ are salaried employees and stockholders of Certara LL was a salaried employee and stockholder of Certara during the execution of the study presented in this manuscript and now is a salaried employee of Daiichi Sankyo. Author GR was employed by F Hoffmann-La Roche Ltd.

## Publisher's note

All claims expressed in this article are solely those of the authors and do not necessarily represent those of their affiliated organizations, or those of the publisher, the editors and the reviewers. Any product that may be evaluated in this article, or claim that may be made by its manufacturer, is not guaranteed or endorsed by the publisher.

## Supplementary material

The Supplementary Material for this article can be found online at: <https://www.frontiersin.org/articles/10.3389/fphar.2022.974423/full#supplementary-material>

- Deng, R., Bumbaca, D., Pastuskovas, C. V., Boswell, C. A., West, D., Cowan, K. J., et al. (2016). Preclinical pharmacokinetics, pharmacodynamics, tissue distribution, and tumor penetration of anti-PD-L1 monoclonal antibody, an immune checkpoint inhibitor. *MAbs* 8, 593–603. doi:10.1080/19420862.2015.1136043
- Edginton, A. N., Schmitt, W., and Willmann, S. (2006). Development and evaluation of a generic physiologically based pharmacokinetic model for children. *Clin. Pharmacokinet.* 45, 1013–1034. doi:10.2165/00003088-200645100-00005
- EMA (2021). *Summary of product characteristics (SmPC) of atezolizumab.*
- FDA (2021). *U.S. prescribing information (USPI) of Atezolizumab.*
- Georger, B., Zwaan, C. M., Marshall, L. V., Michon, J., Bourdeaut, F., Casanova, M., et al. (2020). Atezolizumab for children and young adults with previously treated solid tumours, non-hodgkin lymphoma, and hodgkin lymphoma (IMATRIX): A multicentre phase 1-2 study. *Lancet. Oncol.* 21, 134–144. doi:10.1016/S1470-2045(19)30693-X
- Germovsek, E., Cheng, M., and Giragossian, C. (2021). Allometric scaling of therapeutic monoclonal antibodies in preclinical and clinical settings. *MAbs* 13, 1964935. doi:10.1080/19420862.2021.1964935
- Gill, K. L., Gardner, I., Li, L., and Jamei, M. (2016). A bottom-up whole-body physiologically based pharmacokinetic model to mechanistically predict tissue distribution and the rate of subcutaneous absorption of therapeutic proteins. *AAPS J.* 18, 156–170. doi:10.1208/s12248-015-9819-4
- Grimstein, M., Yang, Y., Zhang, X., Grillo, J., Huang, S. M., Zineh, I., et al. (2019). Physiologically based pharmacokinetic modeling in regulatory science: An update from the U.S. Food and drug administration's office of clinical pharmacology. *J. Pharm. Sci.* 108, 21–25. doi:10.1016/j.xphs.2018.10.033
- Groisberg, R., Hong, D. S., Behrang, A., Hess, K., Janku, F., Piha-Paul, S., et al. (2017). Characteristics and outcomes of patients with advanced sarcoma enrolled in early phase immunotherapy trials. *J. Immunother. Cancer* 5, 100. doi:10.1186/s40425-017-0301-y
- Haigler, H. T., Mckanna, J. A., and Cohen, S. (1979). Rapid stimulation of pinocytosis in human carcinoma cells A-431 by epidermal growth factor. *J. Cell Biol.* 83, 82–90. doi:10.1083/jcb.83.1.82
- Hanke, N., Kunz, C., Thiemann, M., Fricke, H., and Lehr, T. (2019). Translational PBPK modeling of the protein therapeutic and CD95L inhibitor asunercept to develop dose recommendations for its first use in pediatric glioblastoma patients. *Pharmaceutics* 11, 152. doi:10.3390/pharmaceutics11040152
- Hardiansyah, D., and Ng, C. M. (2018). Effects of the FcRn developmental pharmacology on the pharmacokinetics of therapeutic monoclonal IgG antibody in pediatric subjects using minimal physiologically-based pharmacokinetic modelling. *MAbs* 10, 1144–1156. doi:10.1080/19420862.2018.1494479
- Herbst, R. S., Soria, J. C., Kowanzet, M., Fine, G. D., Hamid, O., Gordon, M. S., et al. (2014). Predictive correlates of response to the anti-PD-L1 antibody MPDL3280A in cancer patients. *Nature* 515, 563–567. doi:10.1038/nature14011
- Huang, W., Czuba, L. C., and Isoherranen, N. (2020). Mechanistic PBPK modeling of urine pH effect on renal and systemic disposition of methamphetamine and amphetamine. *J. Pharmacol. Exp. Ther.* 373, 488–501. doi:10.1124/jpet.120.264994
- Inman, B. A., Longo, T. A., Ramalingam, S., and Harrison, M. R. (2017). Atezolizumab: A PD-L1-blocking antibody for bladder cancer. *Clin. Cancer Res.* 23 (8), 1886–1890. doi:10.1158/1078-0432.CCR-16-1417
- Huang, W., Nakano, M., Sager, J., Ragueneau-Majlessi, I., and Isoherranen, N. (2017). Physiologically based pharmacokinetic model of the CYP2D6 probe atomoxetine: Extrapolation to special populations and drug-drug interactions. *Drug Metab. Dispos.* 45, 1156–1165. doi:10.1124/dmd.117.076455
- Johnson, T. N., and Ke, A. B. (2021). Physiologically based pharmacokinetic modeling and allometric scaling in pediatric drug development: Where do we draw the line? *J. Clin. Pharmacol.* 61 (1), S83–S93. doi:10.1002/jcph.1834
- Johnson, T. N., and Rostami-Hodjegan, A. (2011). Resurgence in the use of physiologically based pharmacokinetic models in pediatric clinical pharmacology: Parallel shift in incorporating the knowledge of biological elements and increased applicability to drug development and clinical practice. *Paediatr. Anaesth.* 21, 291–301. doi:10.1111/j.1460-9592.2010.03323.x
- Johnson, T. N., Rostami-Hodjegan, A., and Tucker, G. T. (2006). Prediction of the clearance of eleven drugs and associated variability in neonates, infants and children. *Clin. Pharmacokinet.* 45, 931–956. doi:10.2165/00003088-200645090-00005
- Johnson, T. N., Small, B. G., and Rowland Yeo, K. (2022). Increasing application of pediatric physiologically based pharmacokinetic models across academic and industry organizations. *CPT. Pharmacometrics Syst. Pharmacol.* 11, 373–383. doi:10.1002/psp4.12764
- Joseph, P. D., Craig, J. C., and Caldwell, P. H. (2015). Clinical trials in children. *Br. J. Clin. Pharmacol.* 79, 357–369. doi:10.1111/bcp.12305
- Li, L., Gardner, I., Dostalek, M., and Jamei, M. (2014). Simulation of monoclonal antibody pharmacokinetics in humans using a minimal physiologically based model. *Aaps J.* 16, 1097–1109. doi:10.1208/s12248-014-9640-5
- Liu, S. N., Marchand, M., Liu, X., Ingle, G., Maiya, V., Graupner, V., et al. (2022). Extension of the alternative intravenous dosing regimens of atezolizumab into combination settings through modeling and simulation. *J. Clin. Pharma.* doi:10.1002/jcph.2074
- Lutz, J. D., Mathias, A., German, P., Pikora, C., Reddy, S., and Kirby, B. J. (2021). Physiologically-based pharmacokinetic modeling of remdesivir and its metabolites to support dose selection for the treatment of pediatric patients with COVID-19. *Clin. Pharmacol. Ther.* 109, 1116–1124. doi:10.1002/cpt.2176
- Luzon, E., Blake, K., Cole, S., Nordmark, A., Versantvoort, C., and Berglund, E. G. (2017). Physiologically based pharmacokinetic modeling in regulatory decision-making at the European Medicines Agency. *Clin. Pharmacol. Ther.* 102, 98–105. doi:10.1002/cpt.539
- Madabushi, R., Benjamin, J. M., Grewal, R., Pacanowski, M. A., Strauss, D. G., Wang, Y., et al. (2019). The US food and drug administration's model-informed drug development paired meeting pilot program: Early experience and impact. *Clin. Pharmacol. Ther.* 106, 74–78. doi:10.1002/cpt.1457
- Mager, D. E., and Krzyzanski, W. (2005). Quasi-equilibrium pharmacokinetic model for drugs exhibiting target-mediated drug disposition. *Pharm. Res.* 22, 1589–1596. doi:10.1007/s11095-005-6650-0
- Malik, P., and Edginton, A. (2018). Pediatric physiology in relation to the pharmacokinetics of monoclonal antibodies. *Expert Opin. Drug Metab. Toxicol.* 14, 585–599. doi:10.1080/17425255.2018.1482278
- Malik, P. R. V., and Edginton, A. N. (2020). Integration of ontogeny into a physiologically based pharmacokinetic model for monoclonal antibodies in premature infants. *J. Clin. Pharmacol.* 60, 466–476. doi:10.1002/jcph.1540
- Malik, P. R. V., and Edginton, A. N. (2019). Physiologically-based pharmacokinetic modeling vs. Allometric scaling for the prediction of infliximab pharmacokinetics in pediatric patients. *CPT. Pharmacometrics Syst. Pharmacol.* 8, 835–844. doi:10.1002/psp4.12456
- Morrissey, K. M., Marchand, M., Patel, H., Zhang, R., Wu, B., Phyllis Chan, H., et al. (2019). Alternative dosing regimens for atezolizumab: An example of model-informed drug development in the postmarketing setting. *Cancer Chemother. Pharmacol.* 84, 1257–1267. doi:10.1007/s00280-019-03954-8
- Naqash, A. R., O'sullivan Coyne, G. H., Moore, N., Sharon, E., Takebe, N., Fino, K. K., et al. (2021). Phase II study of atezolizumab in advanced alveolar soft part sarcoma (ASPS). *J. Clin. Oncol.* 39, 11519. doi:10.1200/jco.2021.39.15\_suppl.11519
- Pan, X., Stader, F., Abduljalil, K., Gill, K. L., Johnson, T. N., Gardner, I., et al. (2020). Development and application of a physiologically-based pharmacokinetic model to predict the pharmacokinetics of therapeutic proteins from full-term neonates to adolescents. *AAPS J.* 22, 76. doi:10.1208/s12248-020-00460-1
- Raj, S., Miller, L. D., and Triozzi, P. L. (2018). Addressing the adult soft tissue sarcoma microenvironment with intratumoral immunotherapy. *Sarcoma* 2018, 9305294. doi:10.1155/2018/9305294
- Rippe, B., and Haraldsson, B. (1987). Fluid and protein fluxes across small and large pores in the microvasculature. Application of two-pore equations. *Acta Physiol. Scand.* 131, 411–428. doi:10.1111/j.1748-1716.1987.tb08257.x
- Shemesh, C. S., Chanu, P., Jansen, K., Wada, R., Rossato, G., Donaldson, F., et al. (2019). Population pharmacokinetics, exposure-safety, and immunogenicity of atezolizumab in pediatric and young adult patients with cancer. *J. Immunother. Cancer* 7, 314. doi:10.1186/s40425-019-0791-x
- Sinha, J., Karatza, E., and Gonzalez, D. (2021). Physiologically-based pharmacokinetic modeling of oxcarbazepine and levetiracetam during adjunctive antiepileptic therapy in children and adolescents. *CPT. Pharmacometrics Syst. Pharmacol.* 11, 225–239. doi:10.1002/psp4.12750
- Stroh, M., Winter, H., Marchand, M., Claret, L., Eppler, S., Ruppel, J., et al. (2017). Clinical pharmacokinetics and pharmacodynamics of atezolizumab in metastatic urothelial carcinoma. *Clin. Pharmacol. Ther.* 102, 305–312. doi:10.1002/cpt.587
- Suzuki, T., Ishii-Watabe, A., Tada, M., Kobayashi, T., Kanayasu-Toyoda, T., Kawanishi, T., et al. (2010). Importance of neonatal FcR in regulating the serum half-life of therapeutic proteins containing the Fc domain of human IgG1: A comparative study of the affinity of monoclonal antibodies and fc-fusion proteins to human neonatal FcR. *J. Immunol.* 184, 1968–1976. doi:10.4049/jimmunol.0903296

Temrikar, Z. H., Suryawanshi, S., and Meibohm, B. (2020). Pharmacokinetics and clinical pharmacology of monoclonal antibodies in pediatric patients. *Paediatr. Drugs* 22, 199–216. doi:10.1007/s40272-020-00382-7

Waldmann, T. A., and Strober, W. (1969). Metabolism of immunoglobulins. *Prog. Allergy* 13, 1–110. doi:10.1159/000385919

Wang, Y., Zhu, H., Madabushi, R., Liu, Q., Huang, S. M., and Zineh, I. (2019). Model-informed drug development: Current US regulatory practice and future considerations. *Clin. Pharmacol. Ther.* 105, 899–911. doi:10.1002/cpt.1363

Wilky, B. A., Trucco, M. M., Subhawong, T. K., Florou, V., Park, W., Kwon, D., et al. (2019). Axitinib plus pembrolizumab in patients with advanced sarcomas including alveolar soft-part sarcoma: A single-centre, single-arm, phase 2 trial. *Lancet. Oncol.* 20, 837–848. doi:10.1016/S1470-2045(19)30153-6

Yellepeddi, V., Rower, J., Liu, X., Kumar, S., Rashid, J., and Sherwin, C. M. T. (2019). State-of-the-Art review on physiologically based pharmacokinetic modeling in pediatric drug development. *Clin. Pharmacokinet.* 58, 1–13. doi:10.1007/s40262-018-0677-y

Zhu, H., Huang, S. M., Madabushi, R., Strauss, D. G., Wang, Y., and Zineh, I. (2019). Model-informed drug development: A regulatory perspective on progress. *Clin. Pharmacol. Ther.* 106, 91–93. doi:10.1002/cpt.1475

Zhu, P., Willmann, S., Zhou, W., Yang, H., Michelson, A. D., McCrindle, B. W., et al. (2021). Dosing regimen prediction and confirmation with rivaroxaban for thromboprophylaxis in children after the fontan procedure: Insights from the phase III UNIVERSE study. *J. Clin. Pharmacol.* 62, 220–231. doi:10.1002/jcph.1966